JOM 23567

A comparative study of the use of triethylammonium salts of the $[Fe_2(CO)_6(\mu\text{-}CO)(\mu\text{-}SR)]^-$ anion in the synthesis of iron–gold clusters. Crystal structures of $[Fe_2(CO)_6(\mu\text{-}CO)(\mu\text{-}S^iPr)(\mu\text{-}AuPPh_3)]$ and $[Fe_2(CO)_5(PPh_3)(\mu\text{-}SEt)_2]$

Esther Delgado and Elisa Hernández

Departamento de Química Inorgánica, Facultad de Ciencias, Universidad Autónoma de Madrid, 28049 Madrid (Spain)

Oriol Rossell and Miquel Seco

Departament de Química Inorgànica, Facultat de Química, Diagonal 647, 08028 Barcelona (Spain)

Enrique Gutiérrez Puebla and Caridad Ruiz

Instituto de Ciencia de los Materiales, Sede D, C.S.I.C, Universidad Complutense, 28040 Madrid (Spain)

(Received December 9, 1992)

Abstract

Salts of the type $(NEt_3H)[Fe_2(CO)_6(\mu\text{-}CO)(\mu\text{-}SR)]$ (R = ^{i}Pr, ^{t}Bu, Ph) react with $[ClAuPPh_3]$ in the presence of $TlBF_4$ to produce the neutral iron–gold clusters $[Fe_2(CO)_6(\mu\text{-}CO)(\mu\text{-}SR)(\mu\text{-}AuPPh_3)]$ (R = ^{i}Pr, **1**; R = ^{t}Bu, **2**; R = Ph, **3**) in high yields. The structure of **1** has been determined by X-ray diffraction methods. Crystals are monoclinic, space group $P2_1/c$, with $a = 11.373(1)$, $b = 14.899(3)$, $c = 17.997(8)$ Å, $\beta = 95.12(2)°$ and $Z = 4$, $R = 0.030$ and $R' = 0.035$ for 3579 unique reflections with $I \geq 2\sigma(I)$. The basic skeleton consists of an Fe_2Au triangle where the Fe–Fe bond is bridged by a carbonyl and a thiolate group. In contrast, the reaction of the salts $(NEt_3H)[Fe_2(CO)_6(\mu\text{-}CO)(\mu\text{-}SR)]$ (R = Et or C_6F_5) with $[ClAuPPh_3]$ does not afford the corresponding mixed iron–gold clusters, and the diiron mono- or di-substituted complexes $[Fe_2(CO)_5(PPh_3)(\mu\text{-}SR)_2]$ (R = Et, **4**; R = C_6F_5, **5**) and $[Fe_2(CO)_4(PPh_3)_2(\mu\text{-}SEt)_2]$ (**6**) are obtained instead. The structure of **4** has been established by single-crystal X-ray diffraction studies. Crystals are triclinic, space group, $P\bar{1}$, with $a = 10.472(4)$, $b = 11.329(2)$, $c = 13.437(2)$ Å, $\alpha = 80.34(2)$, $\beta = 92.62(3)$, $\gamma = 114.46(2)°$, and $Z = 2$, $R = 0.027$ and $R' = 0.030$ for 3732 unique reflections with $I \geq 2\sigma(I)$. The Fe–Fe bond in **4** is almost symmetrically double-bridged by two thiolate ligands and the phosphine group attached to the Fe(1) is *trans* to the iron–iron bond.

1. Introduction

Small transition-metal clusters have received considerable attention and are of current research interest, largely because of their relevance to catalysis despite the growing feeling that they may not be satisfactory models for metal surfaces as originally proposed [1]. In previous communications, we have described the synthesis of several mixed-metal clusters containing an Fe_2Au triangular geometry [2–4] by the reaction of the corresponding iron metallate with $[ClAuPPh_3]$. The iron–iron bond in these complexes is invariably bridged by one carbonyl group and by another ligand, such as a carbonyl [2], a phosphido [3], or an ethenyl group [4], and the geometry of the resulting Fe_2Au triangular skeleton strongly depends on the nature of the bridging ligand. Thus, while the anion $[Fe_2(CO)_6(\mu\text{-}CO)_2(\mu\text{-}AuPPh_3)]^-$ and the neutral cluster $[Fe_2(CO)_6(\mu\text{-}CO)(\mu\text{-}PPh_2)(\mu\text{-}AuPPh_3)]$ adopt an almost symmetric triangular array, the related complex $[Fe_2(CO)_6(\mu\text{-}$

Correspondence to: Dr. E. Delgado.

0022-328X/93/$6.00

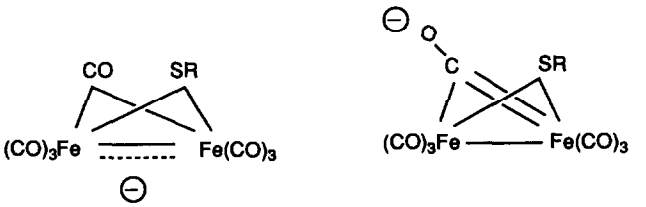

Fig. 1. Resonance forms of bridged thiolate diiron anions.

$CO)(\mu$-PhC=CPh$)(\mu$-$AuPPh_3)]$ exhibits a highly asymmetric triangular system. In the course of our research, we became interested in the use of anions of the type $[Fe_2(CO)_6(\mu$-$CO)(\mu$-$SR)]^-$ as building blocks for the synthesis of new iron–gold clusters given that they would provide interesting structural comparisons with those reported previously. A problem could come from the known ambident nucleophilicity of these anions, as is readily understood on consideration of the resonance hybrid that serves to describe them [5] (Fig. 1); this could perturb the course of the reaction.

However, with the exception of the *O*-alkylation by $[Et_3O][BF_4]$ [6], all reactions of the $[Fe_2(CO)_6(\mu$-$CO)(\mu$-$SR)]^-$ anions can be rationalized in terms of their action as metal-centred nucleophiles. To our knowledge, the only reports of reaction of thiolate anions with metal halides are those with alkyl-, aryl- or vinylmercuric halides [7]. In such processes, although several bimetallic iron–mercury compounds were postulated, no evidence of their formation was obtained. In the present research, we studied the reaction of the anions $[Fe_2(CO)_6(\mu$-$CO)(\mu$-$SR)]^-$ (R = ^{i}Pr, ^{t}Bu, Ph, Et, or C_6F_5) with $[ClAuPPh_3]$ and found that for R = ^{i}Pr, ^{t}Bu and Ph, this leads to mixed iron–gold clusters with a symmetric triangular Fe_2Au unit, according to the X-ray crystal structure of $[Fe_2(CO)_6(\mu$-$CO)(\mu$-$S^iPr)(\mu$-$AuPPh_3)]$. In contrast, no mixed iron–gold clusters are obtained for R = Et or C_6F_5.

2. Results and discussion

The synthesis of salts of the anions $[Fe_2(CO)_6(\mu$-$CO)(\mu$-$SR)]^-$ (R = ^{i}Pr, ^{t}Bu, Ph, Et, or C_6F_5) is achieved by the reaction of a thiol, HSR, with $[Fe_3(CO)_{12}]$ in THF, in the presence of Et_3N [8]. When a molar equivalent of $[ClAuPPh_3]$ and $TlBF_4$ was added to the red-brown $[Et_3NH][Fe_2(CO)_6(\mu$-$CO)(\mu$-$SR)]$ reagent solution, a change to dark green occurred. After stirring for 2 h at room temperature, the solution was filtered through Celite and the solvent then was removed *in vacuo*. After chromatographic workup of the resulting residue, surprisingly, the nature of the final products was shown to depend on the ligand SR. Thus, for R = ^{i}Pr, three products were isolated. The first was the minor, orange $[Fe_2(CO)_6(\mu$-$S^iPr)_2]$. The second, green crystals of $[Fe_2(CO)_6(\mu$-$CO)(\mu$-$S^iPr)(\mu$-$AuPPh_3)]$ (**1**) in 62% yield; and the third, traces of a red product for which the ν(CO) IR pattern is identical to that shown by the trimetallic anion $[Fe_3(CO)_9(\mu$-$S^iPr)]^-$. For R = ^{t}Bu, three similar compounds were obtained: orange $[Fe_2(CO)_6(\mu$-$S^tBu)_2]$; green $[Fe_2(CO)_6(\mu$-$CO)(\mu$-$S^tBu)(\mu$-$AuPPh_3)]$ (**2**) in 66% yield and $[Et_3NH][Fe_3(CO)_9(\mu$-$S^tBu)]$. For R = Ph, only two products were obtained: orange $[Fe_2(CO)_6(\mu$-$SPh)_2]$ and green iron–gold cluster $[Fe_2(CO)_6(\mu$-$CO)(\mu$-$SPh)(\mu$-$AuPPh_3)$ (**3**) in 79% yield. For R = Et or C_6F_5, the resulting solution was red-brown instead of green, and chromatographic workup did not give the corresponding green iron–gold clusters. Thus, when R was Et, the compounds isolated included orange $[Fe_2(CO)_6(\mu$-$SEt)_2]$, red $[Fe_2(CO)_5(PPh_3)(\mu$-$SEt)_2]$ (**4**), and dark red $[Fe_2(CO)_4(PPh_3)_2(\mu$-$SEt)_2]$ (**6**) along with traces of an unidentified red product, whereas for R = C_6F_5, orange $[Fe_2(CO)_6(\mu$-$SC_6F_5)_2]$ and red crystals of $[Fe_2(CO)_5(PPh_3)(\mu$-$SC_6F_5)_2]$ (**5**) were separated.

From these data, it is not easy to rationalize the reactions involving the thiolate anion complexes and the gold derivative. It is obvious that the iron–gold clusters result from electrophilic attack of the $AuPPh_3^+$ cation at the Fe–Fe bond of the iron carbonylmetallate, but why this process occurs only for R = ^{i}Pr, ^{t}Bu and Ph is intriguing. However, we suspect that during the reaction between $[Et_3NH][Fe_2(CO)_6(\mu$-$CO)(\mu$-$SR)]$ (R = Et or C_6F_5) and $[ClAuPPh_3]$, clusters $[Fe_2(CO)_6(\mu$-$CO)(\mu$-$SR)(\mu$-$AuPPh_3)]$ are actually formed. This is because we have occasionally observed a fleeting green colour in the solution that immediately disappears. What is less clear is why the mixed-metal clusters containing the bridging SEt or SC_6F_5 groups are so unstable. Neither electronic nor steric factors clearly explain such different stabilities. On the other hand, the formation in all cases of the undesirable $[Fe_2(CO)_6(\mu$-$SR)_2]$ byproduct is probably due to the fact that the salts $[Et_3NH][Fe_2(CO)_6(\mu$-$CO)(\mu$-$SR)]$ by themselves are not very stable in THF, decomposing with time to $[Fe_2(CO)_6(\mu$-$SR)_2]$ species as reported in an earlier communication [7]. Finally, the formation of $[Fe_2(CO)_5(PPh_3)(\mu$-$SR)_2]$ (R = Et or C_6F_5) and $[Fe_2(CO)_4(PPh_3)_2(\mu$-$SEt)_2]$ can be understood on the basis of a process involving the substitution of one or two carbonyl groups from $[Fe_2(CO)_6(\mu$-$SR)_2]$ by phosphines arising from the fragmentation of the green iron–gold cluster. In fact, bridged thiolate complexes $[Fe_2(CO)_6(\mu$-$SR)_2]$ are known to react in solution with reagents L such as PR_3, $P(OR)_3$, $AsPh_3$, and $SbPh_3$ to afford the substituted derivatives of the type $[Fe_2(CO)_5L(\mu$-$SR)_2]$ [9] and $[Fe_2(CO)_4L_2(\mu$-$SR)_2]$ [10].

TABLE 1. Analytical [a] data and physical parameters of complexes

Compound	Analysis (%)		ν(CO) [b] (cm^{-1})	δ ^{31}P(ppm) [c]	δ ^{1}H NMR [d]
	C	H			
1	40.99 (39.94)	2.69 (2.61)	2050m, 2017s, 1973vs, 1959sh, 1784m	53.3 [b]	1.33 (d, 6H, CH_3, J = 6.26 Hz); 2.22 (m, 1H, CH); 7.48 (m, 15H, PPh_3)
2	40.68 (40.69)	2.80 (2.80)	2048m, 2014s, 1969vs, 1790m	53.2 [b]	1.23 (s, 9H, CH_3); 7.39 (m, 15H, PPh_3)
3	42.69 (42.50)	2.50 (2.28)	2052m, 2022s, 1978vs 1970sh, 1782m	56.7 [b]	7.19 (m, 5H, Ph); 7.50 (15H, PPh_3)
4	51.36 (50.99)	4.21 (3.93)	2041s, 1982vs, 1972sh, 1960sh, 1929w	61.0 [b]	0.99 (2t, 6H, CH_3, J = 7.32 Hz); 2.17 (m, 2H, CH_2); 1.89 (m, 2H, CH_2); 7.41 (m, 15H, PPh_3)
5	46.58 (46.05)	1.94 (1.64)	2058m, 2009vs, 1997s, 1981m, 1944w	66.4 [e]	7.45 (m, 15H, PPh_3)
6	61.71 (61.16)	4.80 (5.10)	1988vs, 1944m, 1919s	44.7 [b]	0.73 (t, 3H, CH_3 J = 7.14 Hz); 2.01 (m, 2H, CH_2); 7.36 (m, 15H, PPh_3)

[a] Required values are given in parentheses. [b] In THF solution. [c] Relative to H_3PO_4. [d] Relative to tetramethylsilane. [e] In $CDCl_3$ solution.

The new complexes were characterized by elemental analysis as well as by IR, ^{1}H, ^{31}P (Table 1), ^{13}C, ^{19}F NMR (see Experimental section), and FAB mass spectroscopy (Table 2). The structures of **1** and **4** were determined by X-ray diffraction. We first discuss the characterization of the gold–iron clusters **1–3** and then of the dinuclear iron compounds.

The ν(CO) IR pattern of **1–3** in THF solutions is practically superimposable on that recorded for the complex $[Fe_2(CO)_6(\mu\text{-}CO(\mu\text{-}PPh_2)(\mu\text{-}AuPPh_3)]$ [3]. This is not surprising given the similarity between the bridging PPh_2 and SR groups, both acting as three-electron donors. The ν(CO) band near 1780 cm^{-1} indicates a μ-CO. ^{1}H and ^{13}C NMR spectra reveal the presence of the organic and carbonyl groups. The ^{31}P NMR spectra of their THF solutions at low temperature are very simple and consist of one signal at about 54 ppm due to the phosphine. The NMR data show the strong tendency of these clusters to fragmentation. For example, when a solution of **2** is allowed to reach room temperature, along with the original signal at 53.2 ppm, new signals appear at 34 and 42.2 ppm, in a non-reversible process, indicating partial cluster decomposition.

The FAB mass spectra of **1–6** were recorded using NBA as the matrix (Table 2). In the spectra of the positive ions, the molecular ion signal, although weak, is always present. The spectra are nearly matrix-free and display signals arising basically from the loss of several carbonyl groups. The $Fe_2(CO)_5(\mu\text{-}SR)$ and $AuPPh_3$ fragments were seen in the FAB mass spectrum of **2** as a result of the fragmentation of the starting metal cluster.

The ^{57}Fe Mössbauer spectrum of **1** also confirms the proposed structure. Thus, the spectrum shows the expected quadrupole doublet (1.35 mm/s) with an isomer shift at 80 K of −0.130 mm/s, in agreement with the presence of only one type of iron atom.

Diffraction-quality crystals of $[Fe_2(CO)_6(\mu\text{-}CO)(\mu\text{-}S^{i}Pr)(\mu\text{-}AuPPh_3)]$ (**1**) were obtained by diffusion of hexane into a THF solution at −20°C. A perspective view of the molecule is shown in Fig. 2.

Significant bond distances and angles are listed in Table 3. The core of the molecule consists of a trinuclear cluster of two iron atoms and one gold atom at the corners of an almost equilateral triangle. The Fe–Fe bond is bridged by both an iso-propyl thiolate ligand (Fe(1)–S and Fe(2)–S bond distances being al-

TABLE 2. FAB mass spectra of the complexes [a]

1	842 (M^+); 459 ($AuPPh_3$); 721 ($Au(PPh_3)_2$); 994 ($Au_2RS(PPh_3)_2$); 1265 ($Au_3(RS)_2(PPh_3)_2$
2	856 (M^+); 772 ($M^+ - 3CO$); 744 ($M^+ - 4CO$); 716 ($M^+ - 5CO$); 688 ($M^+ - 6CO$); 660 ($M^+ - 7CO$); 459 ($AuPPh_3$); 341 ($Fe_2(CO)_5(\mu\text{-}SR)$; 1008 ($Au_2RS(PPh_3)_2$)
3	876 (M^+); 764 ($M^+ - 4CO$); 736 ($M^+ - 5CO$); 680 ($M^+ - 7CO$); 459 ($AuPPh_3$); 721 ($Au(PPh_3)_2$); 1027 ($Au_2RS(PPh_3)_2$); 1333 ($Au_3(RS)_2(PPh_3)_2$)
4	636 (M^+); 580, 552, 524, 496 ($M^+ - nCO$, n = 2–5); 262 (PPh_3)
5	912 (M^+); 856 ($M^+ - 2CO$); 771 ($M^+ - 5CO$); 262 (PPh_3)
6	870 (M^+); 786 ($M^+ - 3CO$); 758 ($M^+ - 4CO$); 580 ($M^+ - 2PPh_3$); 262 (PPh_3)

[a] Matrix: 3-nitrobenzylalcohol (NBA).

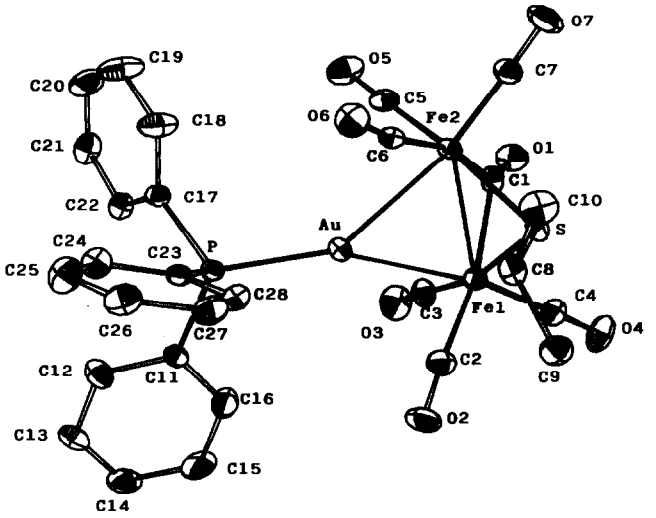

Fig. 2. Molecular structure of $[Fe_2(CO)_6(\mu\text{-}CO)(\mu\text{-}S^iPr)(\mu\text{-}AuPPh_3)]$ (1) including the atom-numbering scheme.

most identical) and a carbonyl group so that both iron atoms attain an 18-electron configuration, with the SR group functioning as a three-electron donor. In addition, the gold atom is coordinated by a triphenylphosphine ligand and three terminal CO groups are attached to each iron atom. The coordination about each iron atom is approximately octahedral (neglecting Fe–Fe bonding). The distortion of the octahedral environment is shown by the angles with the *cis*-coordinated atoms, in the range 72.3(3)–100.4° for Fe(1) and 71.2(3)–96.8(3)° for Fe(2) and with *trans*-coordinated atoms, the smallest being 165.7(3)° for Fe(1) and 165.7(4)° for Fe(2). The Fe–Fe distance in **1**, 2.621(2) Å, is in good agreement with those found between the bridged iron atoms in $[Fe_2(CO)_6(\mu\text{-}CO)_2(\mu\text{-}PPh_2)(\mu\text{-}CuPPh_3)]$ (2.627(1) Å) [3], $[Fe_2(CO)_6(\mu\text{-}CO)(\mu\text{-}PhC{=}CPh)(\mu\text{-}AuPPh_3)]$ (2.600(3)Å) [4], and $[Fe_2(CO)_6(\mu\text{-}CO)(\mu, \eta^2\text{-}SC_{11}H_{19})(\mu\text{-}AuPPh_3)]$ (2.656(1) Å) [11]. On the other hand, the iron–gold distances in **1**, 2.644(1) and 2.695(1) Å, compare well with those reported for the anion $[Fe_2(CO)_6(\mu\text{-}CO)_2(\mu\text{-}AuPPh_3)]^-$ (2.622(1) and 2.698(1) Å) [2] but they are longer than those found in the $[Fe_2Au_2(CO)_8(\mu\text{-dppm})]$ (2.534(2) and 2.527(2) Å) [12].

Red binuclear complexes $[Fe_2(CO)_5(PPh_3)(\mu\text{-}SR)_2]$ (R = Et, **4**; R = C_6F_5, **5**) can exist as two isomers, one containing inequivalent or *anti*-sulphur-ethyl (or pentafluorophenyl) groups and the other showing equivalent or *syn*-sulphur-organic radicals groups. The reports of the analogous derivative $[Fe_2(CO)_5(PPh_3)(\mu\text{-}SMe)_2]$ showed that the ν(CO) IR pattern of the *anti*-isomer consists of five bands, whereas the most symmetric *syn*-isomer exhibits only four bands [13]. In our case, the presence of five bands may indicate that the species in solution is probably the *anti*-isomer, although the *syn*-form cannot be ruled out. The ^{1}H NMR spectrum of **4** seems to confirm this interpretation. Thus, for example, two multiplet signals centred at 2.17 and 1.89 ppm (Table 1) are assigned to the S–CH_2 moieties of the two symmetrically different thiolate ligands of the *anti*-isomer. The ^{13}C NMR

TABLE 3. Selected bond lengths (Å) and angles (°) with estimated standard deviations in parentheses for $[Fe_2(CO)_6(\mu\text{-}CO)(\mu\text{-}S^iPr)(\mu\text{-}AuPPh_3)]$ (1)

Au–Fe1	2.644(1)	S–C8	1.841(9)
Au–Fe2	2.695(1)	P–C11	1.822(8)
Au–P	2.287(2)	P–C17	1.810(8)
Fe1–Fe2	2.621(2)	P–C23	1.816(8)
Fe1–S	2.270(2)	O1–C1	1.172(11)
Fe1–C1	2.016(9)	O2–C2	1.130(13)
Fe1–C2	1.841(10)	O3–C3	1.136(12)
Fe1–C3	1.786(10)	O4–C4	1.138(13)
Fe1–C4	1.786(10)	O5–C5	1.140(12)
Fe2–S	2.263(2)	O6–C6	1.158(12)
Fe2–C1	1.937(9)	O7–C7	1.148(13)
Fe2–C5	1.782(10)	C8–C9	1.527(14)
Fe2–C6	1.805(9)	C8–C10	1.529(13)
Fe2–C7	1.754(10)		
Fe2–Au–P	143.28(6)	C6–Fe2–C7	99.3(4)
Fe1–Au–P	157.91(6)	C5–Fe2–C7	92.7(4)
Fe1–Au–Fe2	58.80(4)	C5–Fe2–C6	91.6(4)
Au–Fe1–C4	168.5(3)	C1–Fe2–C7	94.9(4)
Au–Fe1–C3	78.9(3)	C1–Fe2–C6	165.7(4)
Au–Fe1–C2	72.3(3)	C1–Fe2–C5	88.3(4)
Au–Fe1–C1	94.4(3)	S–Fe2–C7	93.9(3)
Au–Fe1–S	95.02(7)	S–Fe2–C6	96.8(3)
Au–Fe1–Fe2	61.57(4)	S–Fe2–C5	168.2(3)
C3–Fe1–C4	93.0(4)	S–Fe2–C1	81.4(3)
C2–Fe1–C4	100.4(4)	Fe1–S–Fe2	70.66(8)
C2–Fe1–C3	94.0(5)	Fe2–S–C8	112.0(3)
C1–Fe1–C4	93.4(4)	Fe1–S–C8	115.0(3)
C1–Fe1–C3	87.9(4)	Au–P–C23	112.9(3)
C1–Fe1–C2	165.9(4)	Au–P–C17	111.5(3)
S–Fe1–C4	94.6(3)	Au–P–C11	116.3(3)
S–Fe1–C3	165.7(3)	C17–P–C23	104.6(4)
S–Fe1–C2	96.5(3)	C11–P–C23	104.2(4)
S–Fe1–C1	79.6(3)	C11–P–C17	106.3(4)
Fe2–Fe1–C4	129.6(3)	Fe2–C1–O1	140.9(7)
Fe2–Fe1–C3	111.6(3)	Fe1–C1–O1	135.8(7)
Fe2–Fe1–C2	119.8(3)	Fe1–C1–Fe2	83.0(3)
Fe2–Fe1–C1	47.2(3)	Fe1–C2–O2	172.9(9)
Fe2–Fe1–S	54.54(7)	Au–C2–O2	118.1(8)
Au–Fe2–Fe1	59.63(4)	Au–C2–Fe1	67.6(3)
Fe1–Fe2–C7	132.0(3)	Fe1–C3–O3	176.5(9)
Fe1–Fe2–C6	118.0(3)	Fe1–C4–O4	177.6(9)
Fe1–Fe2–C5	113.9(3)	Fe2–C5–O5	178.4(9)
Fe1–Fe2–C1	49.8(3)	Fe2–C6–O6	171.4(7)
Fe1–Fe2–S	54.80(7)	Au–C6–O6	116.4(6)
Au–Fe2–C7	168.4(3)	Au–C6–Fe2	69.9(3)
Au–Fe2–C6	71.2(3)	Fe2–C7–O7	177.9(9)
Au–Fe2–C5	81.2(3)	C10–C8–S	107.5(6)
Au–Fe2–C1	94.8(3)	S–C8–C9	109.8(6)
Au–Fe2–S	93.81(7)	C10–C8–C9	111.3(8)

spectrum of **4** corroborates this assignment (see Experimental section).

In order to confirm the structure, X-ray analysis was carried out on a single crystal obtained by slow diffusion of hexane into a THF solution of **4**. The numbering and the ORTEP representation of the molecule are shown in Fig. 3. Key bond lengths and important bond angles are given in Table 4.

The Fe–Fe bond in **4** appears to be almost symmetrically double-bridged by two thiolates with ethyl groups *anti* to each other. The Fe–Fe bond distance of 2.5242(9) Å is similar to that found for $[Fe_2(CO)_6(\mu\text{-}SEt)_2]$ (2.537(10) Å) [14], but shorter than some reported for similar systems. For example, the Fe–Fe distance is 2.589(1) Å in $[Fe_2(CO)_6(\mu\text{-}CH_3CO_2)(\mu\text{-}S^tBu)]$ [7] and 2.675(1) Å in $[Fe_2(CO)_6(\mu\text{-}C_3H_6)(\mu\text{-}SEt)]$ [15]. In **4**, both iron atoms display a roughly octahedral environment. Interestingly, the phosphine attached to Fe(1) occupies an "apical" coordination site *trans* to the Fe–Fe bond. This basic geometry is in good agreement with that proposed, on the basis of spectroscopic measurements only, for the similar derivatives $[Fe_2(CO)_5(PR'_3)(SR)_2]$ (R = CH_3 or C_2H_5; R' = ^nBu or C_6H_5) [16]. The infrared spectrum of the bis-substituted complex $[Fe_2(CO)_4(PPh_3)_2(\mu\text{-}SEt)_2]$ (**6**) shows a similar band pattern in the carbonyl stretching region to that reported for the complexes $[Fe_2(CO)_4L_2(\mu\text{-}SR)_2]$ (L = tertiary phosphine or phosphite) [17]. The three peaks are consistent with a structure in which the carbonyl groups *trans* to the metal–metal bond in $[Fe_2(CO)_6(\mu\text{-}SR)_2]$ have been replaced by phosphines. Although mixtures of the *syn*- and *anti*-isomers were expected for this derivative, we were able to detect only the *syn*-form from the ^1H and ^{31}P NMR spectra.

TABLE 4. Selected bond lengths (Å) and angles (°) with estimated standard deviations in parentheses for $[Fe_2(CO)_5(\mu\text{-}SEt)_2(PPh_3)]$ (**4**)

Fe1–Fe2	2.5242(9)	P–C16	1.832(4)
Fe1–P	2.239(1)	P–C22	1.824(3)
Fe1–S1	2.255(1)	S1–C8	1.826(4)
Fe1–S2	2.280(1)	S2–C6	1.835(3)
Fe1–C1	1.758(3)	O1–C1	1.147(4)
Fe1–C2	1.762(3)	O2–C2	1.149(4)
Fe2–S1	2.262(1)	O3–C3	1.139(7)
Fe2–S2	2.267(1)	O4–C4	1.138(4)
Fe2–C3	1.796(5)	O5–C5	1.147(5)
Fe2–C4	1.769(3)	C6–C7	1.508(6)
Fe2–C5	1.764(4)	C8–C9	1.513(7)
P–C10	1.830(3)		
C1–Fe1–C2	92.3(2)	S2–Fe2–C3	103.4(1)
S2–Fe1–C2	86.9(1)	S1–Fe2–C5	92.7(1)
S2–Fe1–C1	158.4(1)	S1–Fe2–C4	155.8(1)
S1–Fe1–C2	156.2(1)	S1–Fe2–C3	103.0(1)
S1–Fe1–C1	92.7(1)	S1–Fe2–S2	80.06(5)
S1–Fe1–S2	79.93(5)	Fe1–P–C22	116.8(1)
P–Fe1–C2	96.4(1)	Fe1–P–C16	115.6(1)
P–Fe1–C1	96.3(1)	Fe1–P–C10	114.2(1)
P–Fe1–S2	105.21(5)	C16–P–C22	102.7(1)
P–Fe1–S1	106.05(6)	C10–P–C22	104.3(1)
Fe2–Fe1–C2	100.0(1)	C10–P–C16	101.2(2)
Fe2–Fe1–C1	103.0(1)	Fe1–S1–Fe2	67.94(5)
Fe2–Fe1–S2	56.03(4)	Fe2–S1–C8	114.2(1)
Fe2–Fe1–S1	56.17(5)	Fe1–S1–C8	116.2(1)
Fe2–Fe1–P	153.88(4)	Fe1–S2–Fe2	67.44(4)
Fe1–Fe2–C5	100.9(1)	Fe2–S2–C6	111.8(2)
Fe1–Fe2–C4	99.9(1)	Fe1–S2–C6	117.7(1)
Fe1–Fe2–C3	150.8(1)	Fe1–C1–O1	178.3(3)
Fe1–Fe2–S2	56.52(4)	Fe1–C2–O2	177.8(3)
Fe1–Fe2–S1	55.90(5)	Fe2–C3–O3	177.6(4)
C4–Fe2–C5	91.5(2)	Fe2–C4–O4	179.1(4)
C3–Fe2–C5	100.0(2)	Fe2–C5–O5	177.8(4)
C3–Fe2–C4	99.6(2)	S2–C6–C7	109.3(3)
S2–Fe2–C5	156.5(1)	S1–C8–C9	110.2(3)
S2–Fe2–C4	86.6(1)		

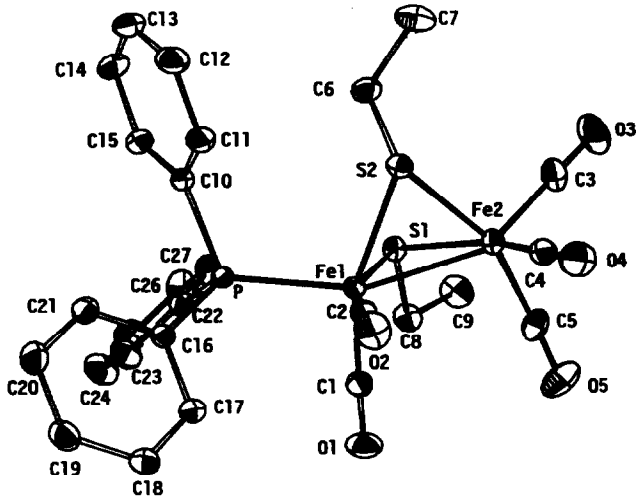

Fig. 3. Molecular structure of $[Fe_2(CO)_5(\mu\text{-}SEt)_2(PPh_3)]$ (**4**) including the atom-numbering scheme.

In conclusion, in this paper we have shown the use of the diiron thiolate anions $[Fe_2(CO)_6(\mu\text{-}CO)(\mu\text{-}SR)]^-$ as building blocks for the synthesis of mixed metal clusters. Further studies are in progress in order to gain insight into the influence of the thiolate groups on the stability of the resulting metal clusters.

3. Experimental details

All reactions were carried out under an atmosphere of prepurified N_2 using Schlenk techniques. Solvents were dried by standard methods. Elemental analyses of C and H were carried out with a Perkin-Elmer 2400 microanalyser. Proton, $^{19}F\text{-}\{^1H\}$, $^{31}P\text{-}\{^1H\}$ and $^{13}C\text{-}\{^1H\}$ NMR spectra were recorded on Bruker AMX 300, Varian Unity 300, Bruker WP 80SY and Bruker AC

300 spectrometers, respectively. Infrared spectra (range 4000–200 cm^{-1}) were recorded on a Nicolet 5 DX FT spectrophotometer. The FAB positive ion mass spectra were recorded on a VG Autospec spectrometer. The Mössbauer spectrum was recorded using 20 mCi of a ^{57}Co source in a Rh matrix, and the calibration was with iron foil. $ClAuPPh_3$ [18] and THF solutions of $(Et_3NH)[Fe_2(CO)_6(\mu\text{-}CO)(\mu\text{-}RS)]$ [8] were prepared as described previously.

3.1. Standard in situ preparation of $[Et_3NH][Fe_2(CO)_6(\mu\text{-}CO)(\mu\text{-}SR)]$

A 100-ml Schlenk flask equipped with a stirrer bar was loaded with 1.0 g (1.98 mmol) of $Fe_3(CO)_{12}$ and degassed by evacuation/dinitrogen-backfill cycles. The flask then was charged with 20 cm^3 of THF, 0.28 cm^3 (1.98 mmol) of triethylamine, and 1.98 mmol of the appropriate thiol. The mixture was stirred for 10 min at room temperature, during which time slow gas evolution and a gradual change from green to brown-red were observed. The resulting $[Et_3NH][Fe_2(CO)_6(\mu\text{-}CO)(\mu\text{-}RS)]$ reagent solution then was utilized *in situ* without further purification.

3.2. Preparation of complexes $[Fe_2(CO)_6(\mu\text{-}CO)(\mu\text{-}SR)(\mu\text{-}AuPPh_3)]$ ($R = {}^iPr$ 1; ^tBu 2; Ph 3)

Details of the synthesis of **1** also apply to **2** and **3**. To a THF solution of $[Et_3NH][Fe_2(CO)_6(\mu\text{-}CO)(\mu\text{-}S^iPr)]$, prepared as above, was added 0.98 g (1.98 mmol) of $[ClAuPPh_3]$ and 0.58 g (1.98 mmol) of $TlBF_4$. After being stirred for 2 h at room temperature, the resulting dark green solution was filtered through a pad of Celite, and the solvents were removed *in vacuo*. The resulting residue was chromatographed on silica gel 100. Elution with pentane yielded one orange band, which afforded 0.13 g (0.30 mmol, 15% yield) of $[Fe_2(CO)_6(\mu\text{-}S^iPr)_2]$. Elution with THF/pentane 1:1 gave 1.1 g (1.23 mmol, 62% yield) of one major product, $[Fe_2(CO)_6(\mu\text{-}CO)(\mu\text{-}S^iPr)(\mu\text{-}AuPPh_3)]$ (**1**), which was recrystallized from THF/hexane. ($^{13}C\text{-}\{^1H\}$ NMR (C_6D_6): δ 26.9 (CH_3); 45.5 (CH); 218 (d, 2CO); 211 (s, br, 4CO); 129.4–133.9(PPh_3)). Finally, traces of $(Et_3NH)[Fe_3(CO)_9(\mu\text{-}S^iPr)]$ were obtained from the third red band, eluted with THF. For R = ^{t}Bu, operating as above, the following compounds were isolated: $[Fe_2(CO)_6(\mu\text{-}S^tBu)_2]$ (6% yield); green $[Fe_2(CO)_6(\mu\text{-}CO)(\mu\text{-}S^tBu)(\mu\text{-}AuPPh_3)]$ (**2**) (66% yield) ($^{13}C\text{-}\{^1H\}$ NMR (C_6D_6): δ 32.2 (CH_3); 47.1 (C); 215.3 (s, 2CO); 212.3 (d, 2CO); 208.1 (s, 2CO)); and $[Et_3NH][Fe_3(CO)_9(\mu\text{-}S^tBu)]$ (5% yield). For R = Ph, only two products were formed: orange $[Fe_2(CO)_6(\mu\text{-}SPh)_2]$ (10% yield) and green $[Fe_2(CO)_6(\mu\text{-}CO)(\mu\text{-}SPh)(\mu\text{-}AuPPh_3)]$ (**3**) (79% yield). ($^{13}C\text{-}\{^1H\}$ NMR (C_6D_6): δ 128.0 (s, br, C_6H_5); 216.9 (d, 2CO); 209.9 (s, br, 4CO).

3.3. Reactions of $(Et_3NH)[Fe_2(CO)_6(\mu\text{-}CO)(\mu\text{-}SR)]$ ($R = Et$, C_6F_5) with $ClAuPPh_3$

Following the above procedure, for R = Et or C_6F_5, the resulting solution was brown-red instead of green and the compounds orange $[Fe_2(CO)_6(\mu\text{-}SEt)_2]$ (6% yield), red $[Fe_2(CO)_5(PPh_3)(\mu\text{-}SEt)_2]$ (**4**) (14% yield) ($^{13}C\text{-}\{^1H\}$ NMR (C_6D_6): δ 17.4, 18.0 (CH_3); 32.6, 31.5 (CH_2); 217.1, 216.4, 214.9, 214.7, 211.5, 211.0 (all s, COs); 129.9–137.1 (PPh_3)), and red $[Fe_2(CO)_4(PPh_3)_2(\mu\text{-}SEt)_2]$ (**6**) (25% yield) ($^{13}C\text{-}\{^1H\}$ NMR (C_6D_6): δ 16.9 (CH_3), 30.9 (CH_2), 219.1 (s, br, 1CO), 218.2 (s, br

TABLE 5. Final atomic parameters for $[Fe_2(CO)_6(\mu\text{-}CO)(\mu\text{-}S^iPr)(\mu\text{-}AuPPh_3)]$ (**1**)

Atom	x	y	z	U_{eq} [a]
Au	0.29460(3)	0.21972(2)	0.14166(2)	413(1)
Fe1	0.49788(10)	0.18565(8)	0.08669(7)	396(4)
Fe2	0.46435(10)	0.34588(7)	0.14124(6)	380(4)
S	0.61057(18)	0.25048(14)	0.18247(11)	403(7)
P	0.10841(18)	0.19317(13)	0.17512(12)	363(7)
O1	0.53763(67)	0.34113(45)	−0.01136(36)	686(27)
O2	0.43662(76)	0.01904(50)	0.16474(51)	924(36)
O3	0.33573(70)	0.14568(57)	−0.04421(41)	867(33)
O4	0.69615(69)	0.11465(59)	0.01206(44)	886(34)
O5	0.27279(74)	0.44609(50)	0.05995(42)	821(32)
O6	0.35233(67)	0.37023(49)	0.28181(39)	739(29)
O7	0.61238(77)	0.50471(52)	0.15482(52)	966(38)
C1	0.51509(76)	0.31038(61)	0.04559(50)	499(31)
C2	0.45684(90)	0.08549(68)	0.13841(59)	613(38)
C3	0.39604(83)	0.16250(67)	0.00766(57)	576(36)
C4	0.62061(85)	0.14296(65)	0.04225(53)	555(34)
C5	0.34639(92)	0.40651(60)	0.09226(50)	510(33)
C6	0.39575(75)	0.35374(53)	0.22764(51)	443(29)
C7	0.55502(88)	0.44121(65)	0.15045(54)	560(35)
C8	0.58900(76)	0.20529(63)	0.27551(46)	514(31)
C9	0.65641(94)	0.11708(69)	0.28773(60)	673(39)
C10	0.63337(97)	0.27587(75)	0.33297(48)	702(38)
C11	0.04064(70)	0.08749(53)	0.14350(44)	393(27)
C12	−0.07303(91)	0.06563(69)	0.15742(57)	623(38)
C13	−0.12188(95)	−0.01584(72)	0.13520(63)	662(42)
C14	−0.05806(109)	−0.07460(70)	0.10098(82)	882(53)
C15	0.05548(117)	−0.05525(75)	0.08660(93)	1071(122)
C16	0.10465(92)	0.02718(74)	0.10787(80)	859(51)
C17	0.00684(70)	0.28091(56)	0.14189(42)	413(26)
C18	0.01878(108)	0.36513(67)	0.17266(65)	773(45)
C19	−0.05410(144)	0.43461(75)	0.14555(79)	1003(62)
C20	−0.13741(115)	0.42102(77)	0.08802(75)	817(51)
C21	−0.15021(87)	0.33933(78)	0.05637(53)	632(38)
C22	−0.08002(75)	0.26701(62)	0.08284(47)	501(30)
C23	0.10118(71)	0.19176(48)	0.27553(45)	378(26)
C24	−0.00221(78)	0.20465(62)	0.30772(48)	522(32)
C25	−0.00565(93)	0.19452(70)	0.38464(53)	638(38)
C26	0.09529(95)	0.17293(65)	0.42843(53)	596(36)
C27	0.19869(89)	0.16161(63)	0.39625(54)	567(35)
C28	0.20300(74)	0.17058(57)	0.32032(49)	458(30)

[a] $U_{eq} = 1/3\Sigma_i\Sigma_j U_{ij} a_i^* a_j^* a_i \cdot a_j \times 10^4$.

TABLE 6. Final atomic parameters for $[Fe_2(CO)_5(\mu\text{-}SEt)_2(PPh_3)]$ (4)

Atom	x	y	z	U_{eq} [a]
Fe1	0.26052(4)	−0.11867(4)	−0.27262(3)	340(2)
Fe2	0.21310(5)	0.05739(4)	−0.20955(4)	403(2)
P	0.25690(8)	−0.31975(8)	−0.25966(6)	336(3)
S1	0.04904(8)	−0.14850(8)	−0.21416(6)	412(3)
S2	0.31940(9)	−0.06101(8)	−0.11684(6)	429(3)
O1	0.17801(32)	−0.09511(31)	−0.48184(20)	772(16)
O2	0.55606(27)	0.03013(26)	−0.32958(22)	692(13)
O3	0.10196(38)	0.14952(34)	−0.05650(28)	1067(20)
O4	0.49083(29)	0.27159(27)	−0.24080(22)	760(13)
O5	0.11556(34)	0.16655(33)	−0.39353(26)	979(18)
C1	0.20982(35)	−0.10642(34)	−0.39910(26)	470(15)
C2	0.43979(35)	−0.03081(32)	−0.30685(24)	428(14)
C3	0.14253(41)	0.11129(36)	−0.11573(33)	628(18)
C4	0.38175(38)	0.18841(33)	−0.22831(25)	496(15)
C5	0.15211(38)	0.12377(36)	−0.31992(32)	593(17)
C6	0.20919(40)	−0.17128(37)	−0.00831(26)	571(17)
C7	0.24593(53)	−0.10290(51)	0.08275(31)	869(26)
C8	−0.08430(37)	−0.15767(38)	−0.30871(30)	587(17)
C9	−0.19560(42)	−0.12384(48)	−0.26890(36)	786(23)
C10	0.29463(34)	−0.38606(30)	−0.13360(22)	397(13)
C11	0.41979(37)	−0.31121(35)	−0.09161(26)	509(16)
C12	0.45429(45)	−0.35452(46)	0.00449(30)	664(21)
C13	0.36243(55)	−0.47163(50)	0.05850(29)	740(25)
C14	0.24013(52)	−0.54590(42)	0.01858(29)	712(22)
C15	0.20418(40)	−0.50456(35)	−0.07847(26)	547(16)
C16	0.38889(31)	−0.33226(29)	−0.33713(22)	375(12)
C17	0.43359(38)	−0.25126(33)	−0.43025(24)	482(15)
C18	0.53386(43)	−0.26088(37)	−0.48877(27)	592(18)
C19	0.58967(41)	−0.34962(38)	−0.45580(29)	595(18)
C20	0.54606(41)	−0.43074(37)	−0.36470(29)	584(18)
C21	0.44589(36)	−0.42271(33)	−0.30562(25)	475(15)
C22	0.09432(33)	−0.44939(29)	−0.29227(24)	415(13)
C23	0.08887(41)	−0.52586(39)	−0.36258(30)	638(18)
C24	−0.03897(51)	−0.62377(45)	−0.38504(36)	816(23)
C25	−0.15966(44)	−0.64385(42)	−0.33699(37)	764(21)
C26	−0.15550(40)	−0.56882(40)	−0.26583(38)	745(20)
C27	−0.02991(38)	−0.47165(35)	−0.24330(32)	603(17)

[a] $U_{eq} = 1/3\Sigma_i\Sigma_j U_{ij} a_i^* a_j^* \boldsymbol{a}_i \cdot \boldsymbol{a}_j \times 10^4$.

2CO), 216.0 (s, br, 1CO), 129.0–137.5 (PPh_3)) along with traces of other unidentified red product were eluted. For R = C_6F_5, orange $[Fe_2(CO)_6(\mu\text{-}SC_6F_5)_2]$ (10% yield) and red $[Fe_2(CO)_5(PPh_3)\mu\text{-}SC_6F_5)_2]$ (**5**) (38% yield) (^{19}F-{^1H} NMR (relative to CCl_3F) ($CDCl_3$): δ −125.7 (d, *o*-C_6F_5); −153.5 (t, *p*-C_6F_5); −161.1 (t, *m*-C_6F_5)) were separated.

3.4. Crystallographic section

The crystals were epoxy-resin coated and mounted on an Enraf-Nonius CAD4-F automatic diffractometer. The cell dimensions were refined by least-squares fitting of the θ values of 25 reflections ($1 < \theta < 25°$). There were no appreciable changes in the periodically monitored standard reflections. Intensities were collected using the ω–2θ scan technique. For **1**, 5431 reflections were measured in the range $1 < \theta < 25°$, 3579 of which with $(I) \geq 2\sigma(I)$. For **4**, 5017 reflections were measured in the range $1 < \theta < 25°$, 3732 of which with $(I) \geq 2\sigma(I)$. The intensities were corrected for Lorentz and polarization effects.

3.5. Crystal data

$C_{28}H_{22}AuFe_2O_7PS$ (**1**): $M = 842.2$, monoclinic, $a = 11.373(1)$, $b = 14.899(3)$, $c = 17.997(8)$ Å, $\beta = 95.12(2)°$, $U = 3037.$ (1) Å^3, space group $P2_1/c$, $Z = 4$, $D_c = 1.84$ g cm^{-3}, $F(000) = 1632$, λ(Mo Kα) = 0.71069 Å, μ(Mo Kα) = 59.12 cm^{-1}, room temperature, dark green, air-sensitive crystals. Crystal dimensions: 0.3 × 0.2 × 0.2 mm^3.

$C_{27}H_{25}Fe_2O_5PS_2$ (**4**): $M = 636.3$, triclinic, $a = 10.472(4)$, $b = 11.329(2)$, $c = 13.437(2)$ Å, $\alpha = 80.34(2)$, $\beta = 92.62(3)$, $\gamma = 114.46(2)°$, $U = 1430.$ (1) Å^3, space group $P\bar{1}$, $Z = 2$, $D_c = 1.48$ g cm^{-3}, $F(000) = 652$, λ(Mo Kα) = 0.71069 Å, μ(Mo Kα) = 12.4 cm^{-1}, room temperature, dark red crystals. Crystal dimensions: 0.25 × 0.25 × 0.10 mm^3.

Final fractional coordinates of non-hydrogen atoms for complexes **1** and **4** are listed in Tables 5 and 6, respectively. Scattering factors for neutral atoms and anomalous dispersion corrections for Fe, P and Au (in **4**) were taken from the *International Tables for X-Ray Crystallography* [19]. Both structures were solved by Patterson and Fourier synthesis, and empirical absorption correction [20] was applied at the end of the isotropic refinement. Anisotropic full-matrix least-squares refinement with unit weights minimizing $\Sigma_w[F_o - F_c]^2$ led to $R = 0.039$ (for **1**) and $R = 0.042$ (for **4**). Final refinement with fixed isotropic temperature factors and coordinates for H atoms gave $R = 0.027$ and $R = 0.030$ for complexes **1** and **4**, respectively. No trend in ΔF *vs.* F_o or (sin θ)/λ was observed. A final difference synthesis showed no significant electron density. Most of the calculations were carried out with X-RAY80 [21].

Tables of all bond distances and angles, final hydrogen parameters, anisotropic thermal parameters, and list of structure factors can be obtained from the authors.

Acknowledgement

Financial support of this work was generously provided by DGICYT (Spain) (Project PB90-0055-C02-01). We thank Esther García and Gabriel García for NMR facilities and Rachid Zquiak for recording the ^{57}Fe Mössbauer spectrum.

References

1 E.L. Muetterties, T.N. Rodin, E. Band, C.F. Brucker and W.R. Pretzer, *Chem. Rev., 79* (1979) 91.

2 O. Rossell, M. Seco and P.J. Jones, *Inorg. Chem., 29* (1990) 348.

3 M. Ferrer, R. Reina, O. Rossell, M. Seco and X. Solans, *J. Chem. Soc., Dalton Trans.*, (1991) 347.
4 R. Reina, O. Rossell, M. Seco, J. Ros, R. Yáñez and A. Perales, *Inorg. Chem.*, 30 (1991) 3973.
5 D. Seyferth, G.B. Womack, C.M. Archer, J.P. Fackler Jr. and D.O. Marler, *Organometallics, 8* (1989) 443.
6 D. Seyferth, G.B. Womack, C.M. Archer and J.C. Dewan, *Organometallics, 8* (1989) 430.
7 D. Seyferth, C.M. Archer, D.P. Ruschke, M. Cowie and R.W. Hilts, *Organometallics, 10* (1991) 3363.
8 D. Seyferth, G.B. Womack and J.C. Dewan, *Organometallics, 4* (1985) 398.
9 See, for example, J.A. deBeer, R.J. Haines, R. Greatrex and N.N. Greenwood, *J. Organomet. Chem., 27* (1971) C33; J.A. de Beer and R.J. Haines, *J. Organomet. Chem., 36* (1972) 297.
10 Von W. Hieber and A. Zeidler, *Z. Anorg. Chem., 329* (1964) 92.
11 H. Umland and U. Behrens, *J. Organomet. Chem., 287* (1985) 109.
12 S. Alvarez, O. Rossell, M. Seco, J. Valls, M.A. Pellinghelli and A. Tiripicchio, *Organometallics, 10* (1991) 2309.
13 J.P. Crow and W.R. Cullen, *Can. J. Chem., 49* (1971) 2948.
14 L.F. Dahl and C. Wei, *Inorg Chem., 2* (1963) 328.
15 D. Seyferth, G.B. Womack and J.C. Dewan, *Organometallics, 4* (1985) 398.
16 L. Maresca, F. Greggio, G. Sbrignadello and G. Bor, *Inorg. Chim. Acta, 5* (1971) 667.
17 J.A. de Beer, R.J. Haines, R. Greatrex and N.N. Greenwood, *J. Chem. Soc. A*, (1971) 3271.
18 C. Kowala and J.M. Swan, *Aust. J. Chem., 19* (1966) 547.
19 *International Tables for X-Ray Crystallography*, Vol. 4, Kynoch Press, Birmingham, 1974, pp. 72–98.
20 N. Walker and D. Stuart, *Acta Crystallogr. Sect. A, 39* (1983) 158.
21 J.M. Stewart, *The x-RAY80 System*, Computer Science Centre, University of Maryland, College Park, 1985.